

Data information transfer using complex optical fields: a review and perspective

(Invited Paper)

Jian Wang (王健)*

Wuhan National Laboratory for Optoelectronics, School of Optical and Electronic Information,
Huazhong University of Science and Technology, Wuhan 430074, China

*Corresponding author: jwang@hust.edu.cn

Received December 18, 2016; accepted January 20, 2017; posted online February 13, 2017

Tailored complex optical fields, may find applications in optical manipulation, imaging, microscopy, quantum information processing, and optical communications. Here, we focus on data information transfer for optical communications using complex optical fields. We review recent research progress in complex optical field modulation, multiplexing, and multicasting for data information transfer on different platforms of waveguides, free space, and fiber. Challenges and perspectives are also discussed.

OCIS codes: 060.4510, 050.4865, 060.4080, 060.4230.

doi: 10.3788/COL201715.030005.

One distinct feature of photons and light is their multiple physical dimensions including wavelength/frequency, time, complex amplitude, polarization, and spatial structure, as shown in Fig. 1. Very recently, the spatial structure of light has attracted increasing interest in optical communications to address the emerging capacity crunch^[1]. One typical example exploiting the spatial structure is a twisted light carrying orbital angular momentum (OAM)^[2], which has a spiral phase structure similar to the natural spiral phenomenon (*e.g.*, helical stairs). An OAM-carrying light is one type of complex optical fields. In general, complex optical fields have complex spatial distributions and/or complex temporal waveforms, as shown in Fig. 2. The complex spatial distributions include spatial amplitude such as a Hermite–Gaussian (HG) beam, spatial phase such as an OAM beam, and spatial polarization such as a vector beam, which can be generated by various schemes^[3–9]. The complex temporal waveforms include complex amplitude and other special waveforms. The complex amplitude is well known for advanced modulation formats such as M-ary phase-shift keying (m-PSK) and M-ary quadrature amplitude modulation (m-QAM)^[10]. The tailored complex optical fields may find a wide variety of interesting applications in optical manipulation, imaging, microscopy, quantum information processing, and optical communications on different platforms of waveguides, free space, and fiber^[11–16].

In this Review, we focus on data information transfer using complex optical fields in waveguides, free space, and fiber.

Taking an OAM beam as one example of complex optical fields, as shown in Fig. 3, the typical data information transfer approaches include modulation, multiplexing, and multicasting. Modulation employs different orthogonal OAM states to encode data information which is similar to the widely used complex amplitude modulation (*e.g.*, m-PSK, m-QAM). Multiplexing adopts

different OAM beams as orthogonal carriers to deliver and combine multi-channel data information. Multicasting duplicates data information into multiple copies for multiple end users (*i.e.*, one-to-many communications). Remarkably, not only OAM beams but other complex optical fields can be used for data information transfer by modulation, multiplexing, and multicasting.

First, we discuss complex optical field modulation for data information transfer.

The complex amplitude modulation, has been not only widely used in long-haul optical fiber communications^[17], but applied to metro/access and data center applications^[18,19]. Moreover, chip-scale optical interconnects have also employed complex amplitude modulation for data information transfer^[20–22]. Here one example is shown of chip-scale data information transfer in a compact silicon microring using orthogonal frequency-division multiplexing based on offset QAM (OFDM/OQAM), which is modulated with a 256-QAM. Figure 4 shows scanning electron microscope (SEM) images of a fabricated silicon microring. We demonstrate chip-scale data information

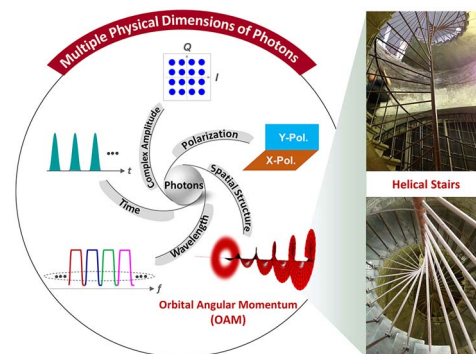


Fig. 1. Multiple physical dimensions of photons and twisted light carrying OAM.

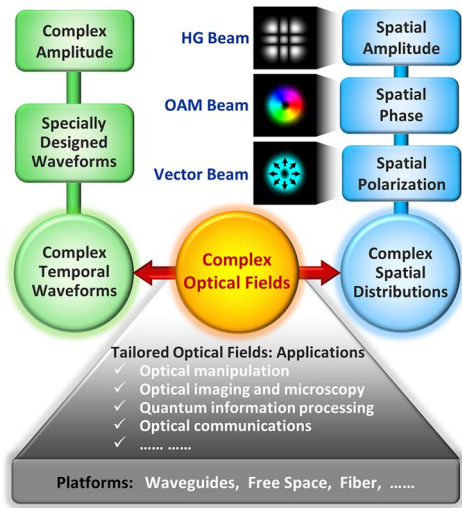


Fig. 2. Classification of complex optical fields and their applications on different platforms.

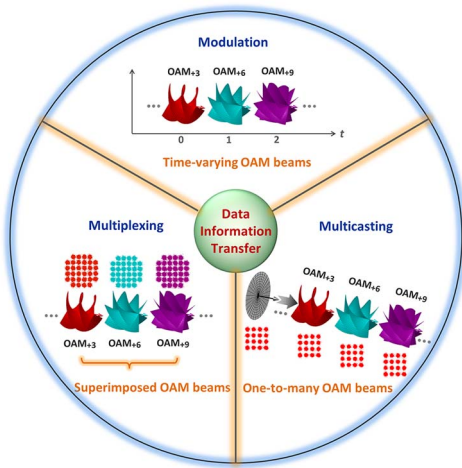


Fig. 3. Illustration of data information transfer using complex optical field modulation, multiplexing and multicasting.

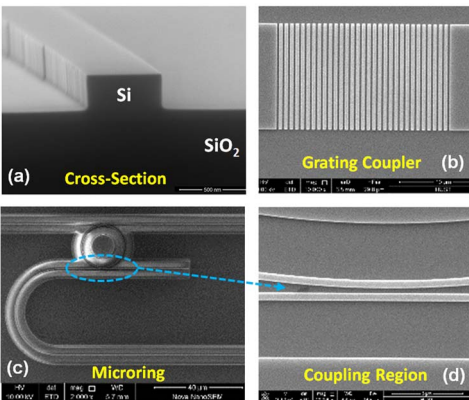


Fig. 4. SEM images of a fabricated silicon microring. (a) Waveguide cross section; (b) grating coupler; (c) microring; (d) coupling region between the bus waveguide and bending waveguide.

transfer of 191.2 Gbit/s eight wavelength OFDM/OQAM 256-QAM signals, as shown in Fig. 5.

Similarly, complex spatial amplitude/phase/polarization modulation can be also used for data information transfer^[23-29]. Here, we show two examples of Bessel beam modulation in free space, and hybrid linearly polarized (LP) mode and OAM mode modulation in fiber.

Shown in Fig. 6 is the concept and principle of high-speed Bessel beam modulation enabling a free-space data information transfer link through turbulence. Although Bessel beams are generated using a commercially available spatial light modulator (SLM) with slow switching response, high-speed operation is achievable by mapping traditional intensity modulation with tens of gigabits speed to spatial modulation. We demonstrate a 20 Gbit/s Bessel beam modulation link in the experiment, as shown in Fig. 7.

Figure 8 shows the concept, principle, and results of spatial mode modulation for data information transfer in fiber. As shown in Fig. 8(a), two spatial modes (OAM_{+1} and OAM_{-1}) can be used to represent binary numbers 0 and 1, while four spatial modes (LP_{01} , LP_{11a} , LP_{11b} , and OAM_{-1}) can be used to denote quaternary numbers 0, 1,

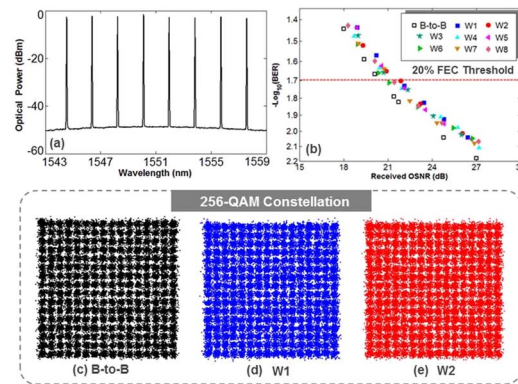


Fig. 5. Measured results of chip-scale data information transfer in a silicon microring using complex amplitude modulation. (a) Spectra of eight wavelength channels (W1-W8); (b) Bit-error rate (BER) versus received optical signal-to-noise ratio (OSNR) for all eight-channel OFDM/OQAM 256-QAM data transmissions; (c)-(e) constellations of 256-QAM signals. B-to-B, back-to-back; FEC, forward error correction.

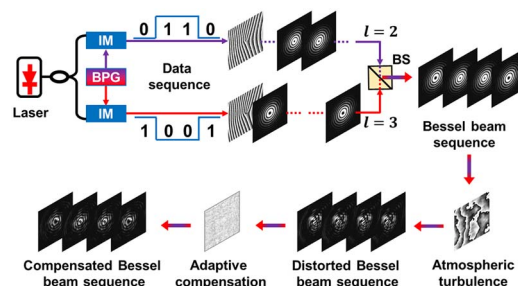


Fig. 6. Concept and principle of high-speed adaptive Bessel beam modulation through turbulence. BPG, bit-pattern generator; IM, intensity modulator; BS, beam splitter.

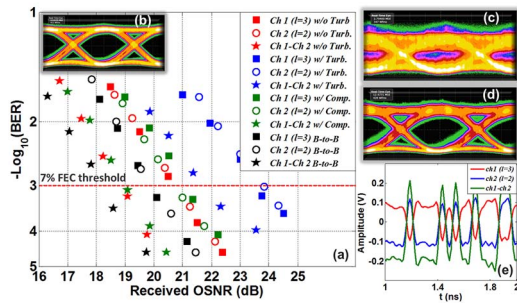


Fig. 7. Measured results of 20 Gbit/s Bessel beam modulation link for free-space data information transfer. (a) BER performance; (b)-(d) eye diagrams; (b) B-to-B; (c) before and (d) after turbulence compensation; (e) temporal waveforms.

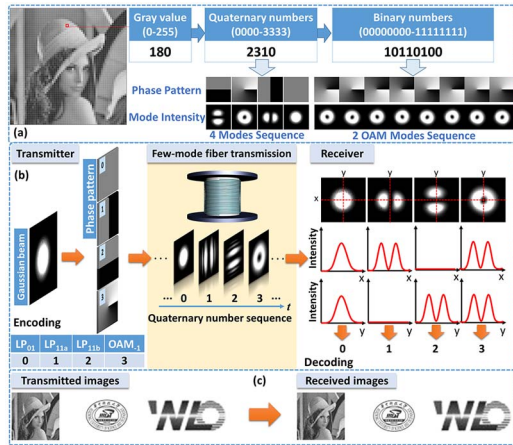


Fig. 8. (a) Concept, (b) principle, and (c) results of spatial mode modulation for data information transfer in fiber.

2, and 3. As shown in Figs. 8(b) and 8(c), by employing four hybrid LP mode and OAM mode modulation, we demonstrate successful image transfer in a 10 km few-mode fiber in the experiment.

Second, we discuss complex optical field multiplexing (e.g., spatial mode multiplexing) for data information transfer.

The spatial mode multiplexing using different mode sets has been reported in waveguides, free space, and fiber^[30-45]. We show here three examples of data-carrying spatial mode multiplexing.

Shown in Fig. 9 are the SEM images of a fabricated silicon mode (de)multiplexer. An asymmetrical directional coupler is employed to enable mode coupling from the fundamental mode (TE_0) in a narrow waveguide to a high-order mode (TE_1 or TE_2) in a wide multi-mode waveguide. Apodized grating couplers are used for light coupling in/out of the chip. We demonstrate chip-scale two- and three-mode (de)multiplexing using OFDM 256-QAM signals with measured bit error rate (BER) performance shown in Fig. 10.

Figure 11 shows the concept of full-duplex data information transfer using OAM multiplexing in an OAM

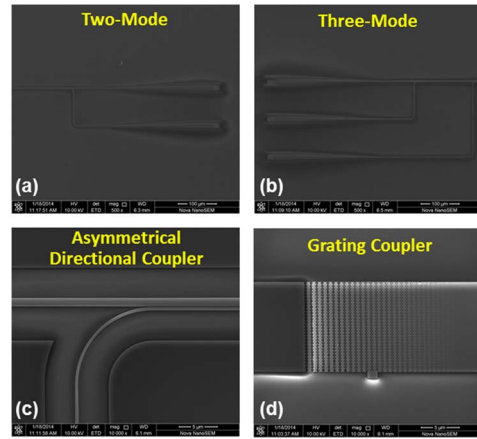


Fig. 9. SEM images of fabricated silicon mode (de)multiplexer. (a) Two-mode; (b) three-mode; (c) asymmetrical directional coupler; (d) grating coupler.

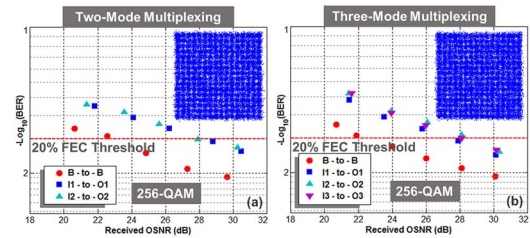


Fig. 10. Measured BER performance and constellations of (a) two-mode and (b) three-mode (de)multiplexing using OFDM 256-QAM signals. I1-I3, input ports; O1-O3, output ports.

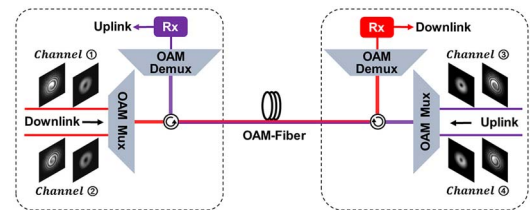


Fig. 11. Concept of full-duplex data information transfer using OAM multiplexing in an OAM fiber.

fiber. The downlink and uplink using x - and y -polarized OAM_{+1} and OAM_{-1} modes share the same OAM fiber link. We demonstrate full-duplex 20 Gbit/s quadrature phase-shift keying (QPSK) data information transfer link using OAM multiplexing through a 1.1 km OAM fiber in the experiment, as shown in Fig. 12. The measured BER performance and constellations are plotted in Fig. 12, showing favorable operation performance.

We further design and fabricate a 50 km OAM fiber for OAM multiplexing data information transfer. Shown in Figs. 13(a) and 13(b) are the relative refractive index profile and a photo of a graded-index 50 km OAM fiber. Shown in Fig. 13(c1)-13(c10) are the measured doughnut-shaped OAM and demodulated Gaussian-like intensity profiles.

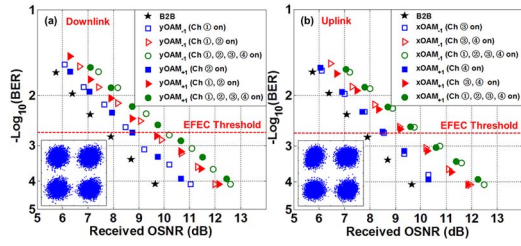


Fig. 12. Measured BER performance and constellations of full-duplex 20 Gbit/s QPSK data information transfer using OAM multiplexing in a 1.1 km OAM fiber. EFEC, enhanced FEC.

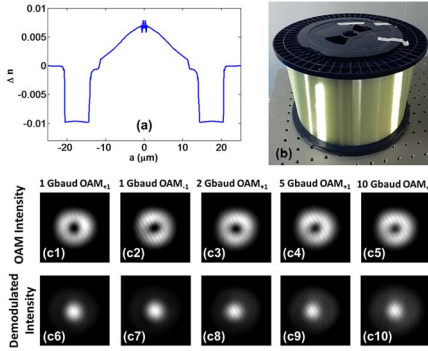


Fig. 13. (a) Relative refractive index profile and (b) photo of OAM fiber. (c1)-(c10) Measured OAM and demodulated Gaussian-like intensity profiles after 50 km fiber transmission.

We demonstrate OAM multiplexing data information transfer in the 50 km OAM fiber, as shown in Fig. 14.

Third, we discuss complex optical field multicasting for data information transfer.

Similar to wavelength multicasting^[46,47], complex optical field multicasting can also be used to facilitate a one-to-many data information transfer^[48–53]. We show here one example of OAM multicasting using a metasurface. Figure 15 presents the on-chip N-fold OAM multicasting using a V-shaped antenna array (metasurface). As shown in Fig. 15(a), an input Gaussian beam is modulated by a V-shaped antenna array, which is designed to be equivalent to a complex multi-OAM phase pattern to generate multiple OAM beams. Inverse phase patterns are used to

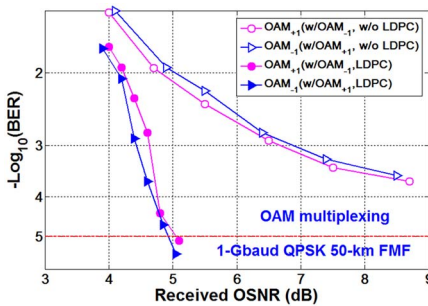


Fig. 14. Measured BER performance of OAM multiplexing data information transfer in the 50 km OAM fiber.

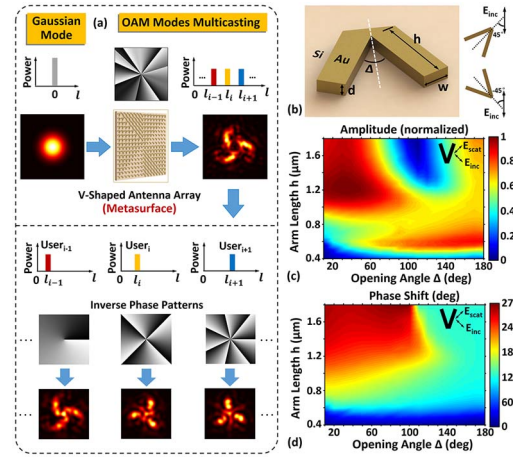


Fig. 15. On-chip N-fold OAM multicasting using V-shaped antenna array (metasurface).

determine the multicasted OAM modes. As shown in Figs. 15(b)–15(d), the V-shaped antenna enables flexible localized spatial amplitude and phase control by proper design of geometric parameters (arm length and opening angle). We achieve on-chip four-fold OAM multicasting with a low crosstalk of less than -15 dB.

In summary, we review of complex optical field modulation, multiplexing, and multicasting for data information transfer on different platforms (waveguides, free space, fiber). More challenges are expected.

For the complex optical field modulation, the challenge would be high-speed spatial mode modulation. Although the modulation mapping scheme shows a simple way to enable a tens of gigabits operation speed^[27,28], it is not straightforward and scalable to a higher base spatial mode modulation. Fast SLM techniques and devices are highly desired.

For complex optical field multiplexing, the challenge would be a (de)multiplexer supporting a large number of spatial modes. Although mode sorters are reported^[54,55], the performance in terms of loss, crosstalk, and scalability to tens of modes still needs to be improved. Robust spatial mode (de)multiplexers are highly desired.

For complex optical field multicasting, the challenge would be the increasing number and flexible control of multicasted channels. Although adaptive power-controllable multicasting is reported^[50], the channel number is still limited. More flexibility and large number spatial mode multicasting techniques are highly desired.

Silicon photonics offers a promising photonic integration platform enabling ultracompact nanophotonic devices for complex optical field manipulation. A long-distance data information transfer link requires turbulence compensation and high-accuracy acquisition, pointing and tracking (APT) techniques in free space, and a specialty fiber supporting a large number of spatial modes. Data information transfer using a conventional graded-index multi-mode fiber could be valuable. Beyond waveguide, free space, and fiber, underwater data information

transfer using complex optical fields would be also interesting.

Overall, the data information transfer using complex optical fields is still an emerging research field. High-speed, high-efficiency, large-scale integration, multi-scale distance, flexibility, and scalability are the trend. Tailored complex optical fields may find more opportunities in future communications and also in noncommunication applications.

This work was supported by the National Basic Research Program of China (No. 2014CB340004), the National Natural Science Foundation of China (NSFC) (No. 11574001), and the National Program for Support of Top-notch Young Professionals.

References

1. D. J. Richardson, J. M. Fini, and L. E. Nelson, *Nat. Photon.* **7**, 354 (2013).
2. L. Allen, M. W. Beijersbergen, R. J. C. Spreeuw, and J. P. Woerdman, *Phys. Rev. A* **45**, 8185 (1992).
3. T. Su, R. P. Scott, S. S. Djordjevic, N. K. Fontaine, D. J. Geisler, X. Cai, and S. J. B. Yoo, *Opt. Express* **20**, 9396 (2012).
4. X. Cai, J. Wang, M. J. Strain, B. J. Morris, J. Zhu, M. Sorel, J. L. O'Brien, M. G. Thompson, and S. Yu, *Science* **338**, 363 (2012).
5. N. Yu, P. Genevet, M. A. Kats, F. Aieta, J. P. Tetienne, F. Capasso, and Z. Gaburro, *Science* **334**, 333 (2011).
6. Z. Zhao, J. Wang, S. Li, and A. E. Willner, *Opt. Lett.* **38**, 932 (2013).
7. L. Zhu and J. Wang, *Sci. Rep.* **4**, 7441 (2014).
8. J. Liu and J. Wang, *Sci. Rep.* **5**, 9959 (2015).
9. S. Li, Q. Mo, X. Hu, C. Du, and J. Wang, *Opt. Lett.* **40**, 4376 (2015).
10. P. J. Winzer, *IEEE LEOS Newsletter* **23**, 4 (2009).
11. S. Franke-Arnold, L. Allen, and M. Padgett, *Laser Photon. Rev.* **2**, 299 (2008).
12. Q. Zhang, *Adv. Opt. Photon.* **1**, 1 (2009).
13. A. Yao and M. J. Padgett, *Adv. Opt. Photon.* **3**, 161 (2011).
14. A. E. Willner, J. Wang, and H. Huang, *Science* **337**, 655 (2012).
15. A. E. Willner, H. Huang, Y. Yan, Y. Ren, N. Ahmed, G. Xie, C. Bao, L. Li, Y. Cao, Z. Zhao, J. Wang, M. P. J. Lavery, M. Tur, S. Ramachandran, A. F. Molisch, N. Ashrafi, and S. Ashrafi, *Adv. Opt. Photon.* **7**, 66 (2015).
16. J. Wang, *Photon. Res.* **4**, B14 (2016).
17. J. Fickers, A. Ghazisaeidi, M. Salsi, G. Charlet, P. Emplit, and F. Horlin, *J. Lightwave Technol.* **32**, 4671 (2014).
18. X. Guo, Q. Wang, X. Li, L. Zhou, L. Fang, A. Wonfor, J. L. Wei, J. von Ledeiner, R. V. Penty, and I. H. White, *Opt. Lett.* **40**, 2353 (2015).
19. J. Wei, N. Eiselt, C. Sanchez, R. Du, and H. Griesser, *Opt. Lett.* **41**, 4122 (2016).
20. L. Xu, W. Zhang, Q. Li, J. Chan, H. L. R. Lira, M. Lipson, and K. Bergman, *IEEE Photon. Technol. Lett.* **24**, 473 (2012).
21. C. Gui, C. Li, Q. Yang, and J. Wang, *Opt. Express* **23**, 9736 (2015).
22. C. Gui and J. Wang, *Photon. Res.* **4**, 168 (2016).
23. G. Gibson, J. Courtial, and M. J. Padgett, *Opt. Express* **12**, 5448 (2004).
24. M. Krenn, R. Fickler, M. Fink, J. Handsteiner, M. Malik, T. Scheidl, R. Ursin, and A. Zeilinger, *New J. Phys.* **16**, 113028 (2014).
25. Y. Zhao and J. Wang, *Opt. Lett.* **40**, 4843 (2015).
26. J. Du and J. Wang, *Opt. Lett.* **40**, 4827 (2015).
27. A. J. Willner, Y. Ren, G. Xie, Z. Zhao, Y. Cao, L. Li, N. Ahmed, Z. Wang, Y. Yan, P. Liao, C. Liu, M. Mirhosseini, R. W. Boyd, M. Tur, and A. E. Willner, *Opt. Lett.* **40**, 5810 (2015).
28. S. Chen, S. Li, Y. Zhao, J. Liu, L. Zhu, A. Wang, J. Du, L. Shen, and J. Wang, *Opt. Lett.* **41**, 4680 (2016).
29. L. Zhu, J. Liu, Q. Mo, C. Du, and J. Wang, *Opt. Express* **24**, 16934 (2016).
30. L. Luo, N. Ophir, C. P. Chen, L. H. Gabrielli, C. B. Poitras, K. Bergmen, and M. Lipson, *Nature Commun.* **5**, 3069 (2014).
31. D. Dai, J. Wang, S. Chen, S. Wang, and S. He, *Laser Photon. Rev.* **9**, 339 (2015).
32. C. Gui, Y. Gao, Z. Zhang, and J. Wang, *IEEE Photon. J.* **7**, 1 (2015).
33. Z. Zhang, X. Hu, and J. Wang, *Sci. Rep.* **5**, 16072 (2015).
34. J. Wang, J.-Y. Yang, I. M. Fazal, N. Ahmed, Y. Yan, H. Huang, Y. X. Ren, Y. Yue, S. Dolinar, M. Tur, and A. E. Willner, *Nat. Photon.* **6**, 488 (2012).
35. G. Milione, M. P. J. Lavery, H. Huang, Y. Ren, G. Xie, T. A. Nguyen, E. Karimi, L. Marrucci, D. A. Nolan, R. R. Alfano, and A. E. Willner, *Opt. Lett.* **40**, 1980 (2015).
36. R. Ryf, S. Randel, A. H. Gnauck, C. Bolle, A. Sierra, S. Mumtaz, M. Esmaelpour, E. C. Burrows, R.-J. Essiambre, P. J. Winzer, D. W. Peckham, A. H. McCurdy, and R. Lingle, *J. Lightwave Technol.* **30**, 521 (2012).
37. N. Bozinovic, Y. Yue, Y. Ren, M. Tur, P. Kristensen, H. Huang, A. E. Willner, and S. Ramachandran, *Science* **340**, 1545 (2013).
38. S. Li and J. Wang, *IEEE Photon. J.* **5**, 7101007 (2013).
39. S. Li and J. Wang, *Sci. Rep.* **4**, 3853 (2014).
40. S. Li and J. Wang, *Opt. Express* **23**, 18736 (2015).
41. H. Huang, G. Milione, M. P. J. Lavery, G. Xie, Y. Ren, Y. Cao, N. Ahmed, T. A. Nguyen, D. A. Nolan, M.-J. Li, M. Tur, R. R. Alfano, and A. E. Willner, *Sci. Rep.* **5**, 14931 (2015).
42. A. Wang, L. Zhu, J. Liu, C. Du, Q. Mo, and J. Wang, *Opt. Express* **23**, 29457 (2015).
43. J. Liu, S. M. Li, J. Du, C. Klitis, C. Du, Q. Mo, M. Sorel, S. Yu, X. Cai, and J. Wang, *Opt. Lett.* **41**, 1969 (2016).
44. J. Liu, L. Zhu, A. Wang, S. Li, S. Chen, C. Du, Q. Mo, and J. Wang, *Opt. Lett.* **41**, 3896 (2016).
45. A. Wang, L. Zhu, S. Chen, C. Du, Q. Mo, and J. Wang, *Opt. Express* **24**, 11716 (2016).
46. A. E. Willner, O. F. Yilmaz, J. Wang, X. Wu, A. Bogoni, L. Zhang, and S. R. Nuccio, *IEEE J. Sel. Top. Quantum Electron.* **17**, 320 (2010).
47. C. Gui and J. Wang, *Sci. Rep.* **4**, 7491 (2014).
48. Y. Yan, Y. Yue, H. Huang, Y. Ren, N. Ahmed, M. Tur, S. J. Dolinar, and A. E. Willner, *Opt. Lett.* **38**, 3930 (2013).
49. L. Zhu and J. Wang, *Opt. Express* **23**, 26221 (2015).
50. S. Li and J. Wang, *Sci. Rep.* **5**, 9677 (2015).
51. L. Zhu and J. Wang, *Opt. Lett.* **40**, 5463 (2015).
52. S. Li and J. Wang, *Opt. Lett.* **41**, 1482 (2016).
53. J. Du and J. Wang, *Sci. Rep.* **5**, 9662 (2015).
54. G. C. G. Berkhout, M. P. J. Lavery, J. Courtial, M. W. Beijersbergen, and M. J. Padgett, *Phys. Rev. Lett.* **105**, 153601 (2010).
55. M. Mirhosseini, M. Malik, Z. Shi, and R. W. Boyd, *Nat. Commun.* **4**, 2781 (2013).